



Nodulisporic acid produces direct activation and positive allosteric modulation of AVR-14B, a glutamate-gated chloride channel from adult *Brugia malayi*

Shivani Choudhary^{a,1}, Melanie Abongwa^{a,1}, Sudhanva S. Kashyap^a, Saurabh Verma^a, Gunnar R. Mair^a, Daniel Kulke^a, Richard J. Martin^a , and Alan P. Robertson^{a,2} 

Edited by Timothy Geary, McGill University, Ste-Anne-de-Bellevue, Canada; received July 14, 2021; accepted June 13, 2022, by Editorial Board Member David J. Mangelsdorf

Glutamate-gated chloride channels (GluCl) are unique to invertebrates and are targeted by macrocyclic lactones. In this study, we cloned an AVR-14B GluCl subunit from adult *Brugia malayi*, a causative agent of lymphatic filariasis in humans. To elucidate this channel's pharmacological properties, we used *Xenopus laevis* oocytes for expression and performed two-electrode voltage-clamp electrophysiology. The receptor was gated by the natural ligand L-glutamate (effective concentration, 50% $[EC_{50}] = 0.4$ mM) and ivermectin (IVM; $EC_{50} = 1.8$ nM). We also characterized the effects of nodulisporic acid (NA) on *Bma*-AVR-14B and NA-produced dual effects on the receptor as an agonist and a type II positive allosteric modulator. Here we report characterization of the complex activity of NA on a nematode GluCl. *Bma*-AVR-14B demonstrated some unique pharmacological characteristics. IVM did not produce potentiation of L-glutamate-mediated responses but instead, reduced the channel's sensitivity for the ligand. Further electrophysiological exploration showed that IVM (at a moderate concentration of 0.1 nM) functioned as an inhibitor of both agonist and positive allosteric modulatory effects of NA. This suggests that IVM and NA share a complex interaction. The pharmacological properties of *Bma*-AVR-14B indicate that the channel is an important target of IVM and NA. In addition, the unique electrophysiological characteristics of *Bma*-AVR-14B could explain the observed variation in drug sensitivities of various nematode parasites. We have also shown the inhibitory effects of IVM and NA on adult worm motility using Worminator. RNA interference (RNAi) knockdown suggests that AVR-14 plays a role in influencing locomotion in *B. malayi*.

glutamate-gated chloride channels | filarial nematode | *Brugia malayi* | nodulisporic acid | AVR-14B

Ligand-gated ion channels (LGICs) are evolutionarily diverse and critical membrane proteins that play a fundamental role in synaptic transmission in metazoans. These aqueous pores generate electrical activity by facilitating transport of specific ions across cell membranes in response to binding of a neurotransmitter, regulating many of the essential biological functions. Parasitic nematodes have a vast repertoire of ion channels belonging to the *cys*-loop LGIC family that are molecular targets of many anthelmintic drugs. The glutamate-gated chloride channels (GluCl) are such anion-selective channels that modulate fast inhibitory neurotransmission at nematode neuronal and neuromuscular synapses (1, 2). These channels are pentameric glycoprotein complexes gated by L-glutamate and are composed of membrane-spanning subunits delineating a central chloride-selective pore. GluCl are confined to invertebrates, including nematodes and arthropods, making them suitable anthelmintic and insecticidal targets (3). These inhibitory receptors are evolutionarily related homologs of mammalian ionotropic glycine channels and γ -amino butyric acid (GABA) channels (2, 4). Functionally, GluCl assist in regulating locomotion, pharyngeal pumping, and sensory processes such as olfaction and temperature responses in *Caenorhabditis elegans* (5–10). GluCl protein complexes can be formed by assembly of a single subunit type or combination of subunits produced by various genes. This can result in receptor subtypes with different pharmacological sensitivities, which is a desired feature in drug discovery (11).

The macrocyclic lactones, which include anthelmintics such as ivermectin (IVM) and moxidectin, target LGICs in invertebrates, with GluCl being primary and relevant targets for their activity (12–14). IVM, introduced by Merck in the 1980s, has been the most successful veterinary parasiticide used for the control of endo- and ectoparasites in animals and agricultural pests (15). It has been a cornerstone of one of the most successful public health programs for the control of human parasitic infections, onchocerciasis (river blindness) and lymphatic filariasis (elephantiasis), providing relief

Significance

Filarial nematodes affect millions of people globally and constitute a serious public health issue in tropical and subtropical regions. Ivermectin (IVM) is used in combination with other chemotherapeutic agents for treatment and control of filarial infections. Glutamate-gated chloride channels (GluCl) are targeted by IVM to produce hyperpolarization and muscle paralysis. This is effective in clearing microfilariae from the host and suppresses their reappearance but has limited adulticidal activity. Here, we functionally expressed and characterized a *Brugia malayi* AVR-14B GluCl channel, investigated the physiological relevance, and elucidated the pharmacological spectrum of the receptor to establish its validity as a drug target. We used electrophysiology and pharmacology to gain a mechanistic understanding of IVM and nodulisporic acid (NA) activity on the channel.

The authors declare no competing interest.

This article is a PNAS Direct Submission. T.G. is a guest editor invited by the Editorial Board.

Copyright © 2022 the Author(s). Published by PNAS. This article is distributed under [Creative Commons Attribution-NonCommercial-NoDerivatives License 4.0 \(CC BY-NC-ND\)](https://creativecommons.org/licenses/by-nc-nd/4.0/).

¹S.C. and M.A. contributed equally to this work.

²To whom correspondence may be addressed. Email: alanr@iastate.edu.

This article contains supporting information online at <http://www.pnas.org/lookup/suppl/doi:10.1073/pnas.2111932119/-DCSupplemental>.

Published August 15, 2022.

to hundreds of millions of people affected globally (16–19). It is a semisynthetic 22,23-dihydroavermectin derivative that was discovered in the fermentation products isolated from the bacterium *Streptomyces avermectilis* (20). It has exceptional potency against an array of nematodes and a preferable safety profile, which stems from its ability to activate invertebrate-specific GluCl α s at nanomolar concentrations and preventing the closure of the channels (21–27). It interacts with GluCl α s in nerve and muscle cells, leading to dampening of neuronal excitation through hyperpolarization of the neuronal membranes, consequently leading to persistent paralysis of the pharyngeal and body wall musculature and death of the parasite (28, 29). Another reason for the exceptional safety of IVM at therapeutic doses in humans is its exclusion from the nervous system by a P-glycoprotein, *mdr-1* (30, 31). This limited penetration of IVM in the brain prevents any potential adverse neurological drug reactions in the host (30, 31).

Various studies have been conducted on GluCl α s from ecdysozoa (nematodes and arthropods) and molluscan lineages. Nematodes possess a small family of genes encoding these anion channels. Cully et al. (21) cloned and expressed the first GluCl subunits, *glc-1* and *glc-2*, from *C. elegans*. This was followed by identification and cloning of additional GluCl-encoding genes from *C. elegans* and other invertebrates, including *Haemonchus contortus*, *Cooperia oncophora*, *Diriofilaria immitis*, *Ascaris suum*, *Drosophila melanogaster*, and *Schistosoma mansoni* (2, 6, 21, 32–35). So far, six *C. elegans* GluCl-encoding genes have been identified: *glc-1* (GluCl α 1), *glc-2* (GluCl β), *glc-3* (GluCl α 4), *glc-4*, *avr-14* (GluCl α 3), and *avr-15* (GluCl α 2) (2, 21, 23, 24, 36, 37). Out of the six genes, *glc-4*, *avr-14*, and *avr-15* are alternatively spliced into multiple variants giving at least nine possible subunits. When expressed heterologously, most of these subunits form a functional homomeric channel that is directly activated by both glutamate and IVM independently, with the exception of GLC-1 and GLC-2 (38). Expression of GLC-1 results in an IVM-sensitive anion channel, while GLC-2 homomeric channels are gated by glutamate but are IVM insensitive. GLC-1 and GLC-2 can coassemble to form IVM-sensitive, glutamate-gated heteromeric receptors. Direct activation of these channels by IVM is slow and irreversible in the time frame of electrophysiology recordings. In addition, IVM and glutamate share allosteric interaction, with IVM potentiating glutamate activity of heteromeric GLC-1/GLC-2 channels (21). While AVR-14 subunits are widely conserved, there is also evidence of variation in the genetics of GluCl α s between species; in particular, *H. contortus* possesses GluCl α (GLC-5) and GLC-6 subunits, which have no orthologs identified in *C. elegans* (27, 39, 40). Heterologously expressed GluCl α s are sensitive to ibotenate, a conformationally constrained analog of glutamate, but are insensitive to candidate or amino acid neurotransmitters such as aspartate, kainate, quisqualate, *N*-methyl-D-aspartic acid (NMDA), α -amino-3-hydroxy-5-methyl-4-isoxazolepropionic acid (AMPA), GABA, glycine, and histamine and are blocked by picrotoxin (PTX) (28, 29). Information regarding the physiological role of GluCl α s in nematodes is limited. However, GluCl α s are expressed in motor neurons and the pharynx in parasitic nematodes, including *H. contortus* and *A. suum* (6, 29, 41, 42). Additionally, treatment of nematodes with IVM results in inhibition of pharyngeal pumping and locomotion. This suggests that GluCl α s have important roles in feeding and locomotion in parasitic species (6, 29, 41, 42).

Nodulisporic acid (NA) is a structurally unique fungal secondary product purified from the fermentation extracts of *Nodulisporium* sp. This indole diterpene is a potent insecticidal compound that was discovered by Merck Research Laboratories in 1992

(43, 44) with no reported antinematodal activity. Smith et al. (45) identified GluCl α s as a target of NA in insects. The fungal diterpene is structurally dissimilar to IVM and shares a comparable mode of action on insect GluCl α s. Unlike IVM, NA is more selective for insect receptor classes as it does not activate vertebrate glycine- or GABA-gated ion chloride channels, conferring a better therapeutic index. In grasshopper neurons, NA was able to bind to and open GluCl α s alone or to potentiate glutamate-mediated channel opening (45). In the same study, high-affinity binding sites for NA were identified in *D. melanogaster* head neurons that were distinct from glutamate-binding sites. The NA- and IVM-binding sites in *Drosophila* were allosterically coupled and shared a complex interaction. While IVM inhibits binding of NA in a competitive fashion, NA inhibited the binding of IVM to *Drosophila* membranes in a biphasic manner. This suggests that IVM can bind to distinct populations of GluCl α receptors, one that also binds NA and the other that does not (45). Ludmerer et al. (46) showed that distinct IVM-binding sites are present on multiple channel complexes. Both NA and IVM can bind to a heteromeric channel composed of GluCl α and Rdl subunits (Resistance to Dieldrin and Lindane locus, a subunit of GABA-gated chloride channels) with high affinity. In addition, IVM has binding sites associated with GluCl α channels. Furthermore, studies of IVM and NA binding on membranes of grasshopper, *Drosophila*, and *C. elegans* from various tissue preparations showed that IVM can bind with high affinity to multiple channel complexes that have variable affinity for NA (45). Also, none of the membrane preparations showed high-affinity NA binding without a corresponding binding site for IVM. This highlights the existence of complex pharmacological interactions of NA and IVM. Both NA and IVM are not only among the most potent compounds for LGICs based on their dissociation constants (pM range), but they also exhibit a good safety profile. Even though they do not share structural similarities, their biological interaction in insects is very intriguing.

GluCl α s from *Brugia malayi*, a causative agent of elephantiasis, are of considerable interest and could have potential as new drug targets for anthelmintic drug development. Investigation of different GluCl subunits from *B. malayi* can provide insights into drug target roles of individual subunits. Understanding the varied drug sensitivities of the filarial GluCl α s is a crucial step in the developmental pipeline for drugs against lymphatic filariasis. Here, we examined the effects of NA, IVM, and GluCl channel knockdown on adult *B. malayi*. We also cloned, functionally expressed, and performed pharmacological characterization of the *B. malayi* AVR-14B GluCl receptor to understand the importance of this channel in the filarial worm. We also explored the pharmacological spectrum of NA activity and its interaction with IVM in the AVR-14B GluCl channel.

Results

IVM and NA Inhibit Adult Filarial Movement. In many species, nematocidal activity is produced through the effects of IVM on the pharyngeal musculature. In filaria, IVM inhibits locomotion, egg production, or release of microfilaria and induces loss of host immunosuppression (10), while effects on the pharynx have not been demonstrated. IVM has predominant microfilaricidal effects, leading to fast and prolonged clearance of microfilariae (mf) but has limited adulticidal activity. We were interested in understanding the in vivo biological effects of the drug on adult filarial motility and used higher-than-recommended therapeutic concentrations in this study. Fig. 1*A* shows the concentration-dependent inhibitory effects of IVM on adult female and male

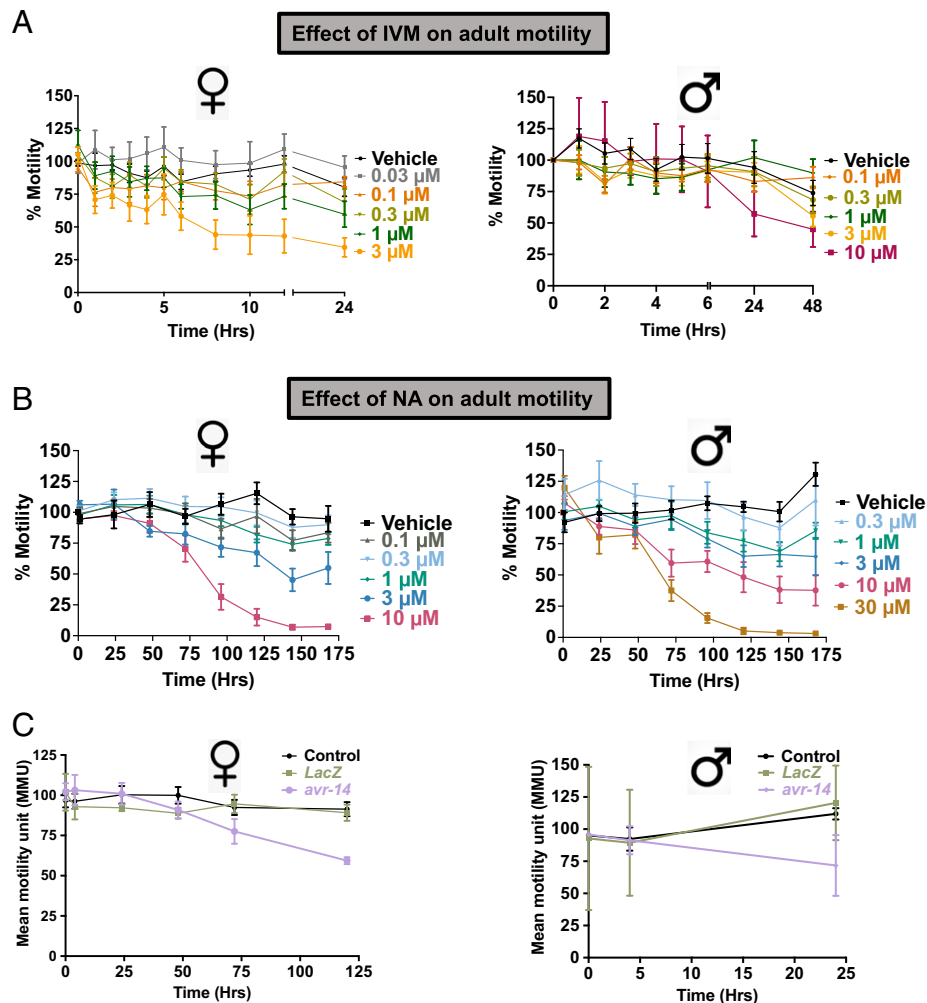


Fig. 1. Effect of IVM and NA on adult worm motility. (A) Time- and concentration-dependent effects of IVM on adult female ($n \geq 10$) and male ($n \geq 10$) *B. malayi* worms in 24-well plates. Motility was recorded with the Worminator system. (B) Time- and concentration-dependent effects of NA on adult female ($n \geq 10$) and male ($n \geq 10$) *B. malayi* worms in 24-well plates. Motility was recorded with the Worminator system. (C) Effect of RNAi knockdown of *Bma-avr-14* on adult worm motility. Time series of motility for dsRNA-soaked adult female ($n = 15$) and male ($n = 15$) worms. Black data points represent untreated control. Error bars represent the SEM.

B. malayi worms. We observed time-, concentration-, and sex-dependent differences in inhibitory effects of IVM in adult worms. At the 24-h time point, the male concentration that inhibits response by 50% (IC_{50}) was 11.6 μM (negative log of molar IC_{50} [pIC_{50}] = 4.9 ± 0.2), while the female IC_{50} was 1.1 μM (pIC_{50} = 5.9 ± 0.4) (SI Appendix, Fig. S1 A and B). The female worms were $\sim 15\times$ more sensitive to the immobilizing effects of IVM in comparison to male worms. We also investigated the biological effects of NA on adult *Brugia* motility (Fig. 1B). As observed with IVM, there were time-, concentration-, and sex-dependent differences in inhibitory effects of NA, with females (IC_{50} = 3.3 μM ; pIC_{50} = 5.5 ± 0.1) being $\sim 2\times$ more sensitive than male worms (IC_{50} = 8.5 μM ; pIC_{50} = 5.1 ± 0.1) (SI Appendix, Fig. S1 C and D). Both NA and IVM produced immobilizing effects in the worms, but NA required a higher concentration and much longer exposure (>3 d) to produce a similar reduction in worm motility. Cook et al. (8) implicated AVR-14 as one of the GluCl subunits that affect forward locomotion. Mutations of *avr-14* produced a deficit in duration of forward movement in *C. elegans*, thus regulating foraging behavior. We knocked down the *avr-14* transcript in *B. malayi* adults and studied its effect on worm motility (Fig. 1C). We were able to achieve $90 \pm 3.9\%$ knockdown in females and $84 \pm 3.1\%$ knockdown in male worms by using *avr-14*-specific double-stranded RNA (dsRNA)

(SI Appendix, Fig. S2 A and B). Only *avr-14*-treated worms showed a reduction in motility in both adult male and female worms in comparison to *lacZ*-treated control worms. The *avr-14* transcript knockdown produced faster reduction in motility (24 h) in males in comparison to females (120 h). This shows that AVR-14 contributed to locomotion in the filarial worms; however, since the observed effect was mild, it is possible that other subunits also participated in the receptors involved in controlling this behavior.

Sequence Comparison of *B. malayi* AVR-14B with *C. elegans* AVR-14B.

We performed a Blast search on the National Center for Biotechnology Information (NCBI) and WormBase databases using *C. elegans* sequences as queries and found sequences for *B. malayi* *glc-2* (WormBase ID: Bm3578), *glc-3* (WormBase ID: Bm8050), *glc-4* (WormBase ID: Bm2442), and *avr-14*. We also found four splice variants of *avr-14* for which there are full lengths for only three of the four *avr-14* isoforms, namely: *Bma-avr-14A* (NCBI GenBank: HQ123446.1, annotated Bm1710c in WormBase), *Bma-avr-14B* (NCBI GenBank: HQ123447.1; annotated Bm1710a in WormBase), and *Bma-avr-14D* (NCBI GenBank: LN856021.1; annotated Bm1710b in WormBase). We amplified and cloned the putative full-length coding sequence of AVR-14B (GenBank: HQ123447.1) from adult female

	Loop G	Loop A	Loop B	Loop C	Loop D	Loop E	Loop F
<i>Cel</i> -AVR-14B	LR S	PD TFFQ N	AS YAY	CTSL TNTGEY SC	FR EEW	LY SVR	QQ KDGLRQ
<i>Bma</i> -AVR-14B	LR S	PD TFFQ N	AS YAY	CTSL TNTGEY SC	FR EEW	LY SVR	QQ KEGLRQ
<i>Hco</i> -AVR-14B	LR S	PD TFFQ N	AS YAY	CTSL TNTGEY SC	FR EEW	LY SVR	QQ KDGLRQ
<i>Dim</i> -AVR-14B	LR S	PD TFFQ N	AS YAY	CTSL TNTGEY SC	FR EEW	LY SVR	QQ KEGLRQ
<i>Con</i> -AVR-14B	LR S	PD TFFQ N	AS YAY	CTSL TNTGEY SC	FR EEW	LY SVR	QQ KDGLRQ

	Pre-TM1	TM1	TM2
<i>Cel</i> -AVR-14B	V VLR LRREYS	YYLIQ LYI FCIMLVVSVSWVFWL	PAR VSLGVT LLTMTTQASGINSK
<i>Bma</i> -AVR-14B	V MLL LRREYS	YYLIQ LYI FCIMLVVSVSWVFWL	PAR VSLGVT LLTMTTQASGINAK
<i>Hco</i> -AVR-14B	V KLL LRREYS	YYLIQ LYI FCIMLVVSVSWVFWL	PAR VSLGVT LLTMTTQASGINSK
<i>Dim</i> -AVR-14B	V MLL LRREYS	YYLIQ LYI FCIMLVVSVSWVFWL	PAR VSLGVT LLTMTTQASGINAK
<i>Con</i> -AVR-14B	V KLL LRREYS	YYLIQ LYI FCIMLVVSVSWVFWL	PAR VSLGVT LLTMTTQASGINSK

	TM2-TM3 Linker	TM3	TM4
<i>Cel</i> -AVR-14B	L PPV SYIK AVDIW IG VCLAFIFGALLEYALVNYY	ISRF AFP TFACFLVLYVYVNVN----	
<i>Bma</i> -AVR-14B	L PPV SYIK AVDVW IG VCLAFIFGALLEYAVVNYY	MSRL TF PLTFFSFLIFYYVAVKQSRD-	
<i>Hco</i> -AVR-14B	L PPV SYIK AVDVW IG VCLAFIFGALLEYAVVNYY	MSRI TF PSLFTAFLVVFYYSVYVQSNLD	
<i>Dim</i> -AVR-14B	L PPV SYIK AVDVW IG VCLAFIFGALLEYALVNYY	ISRF AFP TFFAFLVLYVYVNVN----	
<i>Con</i> -AVR-14B	L PPV SYIK AVDVW IG VCLAFIFGALLEYAVVNYY	LSRR VD LSRI TF PTLFTVFL-----	

Fig. 2. Protein sequence alignment of selected nematode AVR-14B homologs showing ligand-binding loops, transmembrane domain (TM1-TM4), pre-TM1 region, and TM2-TM3 linker region. Residues of the amino acid agonist (AAA) motif that contact bound glutamate are illustrated in maroon. Residues that reduce agonist sensitivity are highlighted in purple in the pre-TM1 and TM2-TM3 linker region. PAR motif, which is characteristic of LGICs, is coded in orange in the TM2 region. The sites of mutation that reduced IVM sensitivity are illustrated in a black box in the TM regions. *Cel*, *C. elegans*; *Bma*, *B. malayi*; *Hco*, *H. contortus*; *Dim*, *D. immitis*; *Con*, *C. oncophora*.

B. malayi worms (SI Appendix, Fig. S3). The protein subunit, AVR-14B, is assembled from 423 amino acids and contains the features common to LGICs, such as a large N-terminal extracellular domain, four transmembrane regions (TM1–TM4), a Cys-loop motif, ligand-binding loops A–G, and a “PAR” motif at the very start of the TM2 region (29, 47, 48). Alignment of various domains of *B. malayi* AVR-14B with selected AVR-14B homologs from *C. elegans* and other parasitic nematodes is shown in Fig. 2. *Bma*-AVR-14B displayed high-level conservation of ligand-binding residues from various loops and transmembrane regions. This suggested that AVR-14B has the potential to express as a functional homomeric channel.

Functional Expression of *B. malayi* AVR-14B in *Xenopus laevis* Oocytes.

Actions of L-glutamate, ibotenate, L-aspartate, glycine, GABA, AMPA, NMDA, kainate, and quisqualate. The application of 1 mM L-glutamate and ibotenate, a structural analog of glutamate, evoked a rapidly activating, reversible, and desensitizing inward membrane current from oocytes expressing *B. malayi* AVR-14B (Fig. 3A). Other glutamate analogs such as L-aspartate, AMPA, NMDA, kainate, and quisqualate failed to induce any measurable channel activity. Glycine and GABA, which are known agonists of vertebrate and invertebrate glycine and GABA channels, respectively, were also inactive on the *Bma*-AVR-14B receptor. The rank order series for agonists was L-glutamate > ibotenate ≫≫ kainate = L-quisqualate = L-aspartate = glycine = GABA = AMPA = NMDA.

Glutamate concentration-response and current-voltage (I-V) relationships. We examined the concentration-response relationship for L-glutamate on the *Bma*-AVR-14B GluCl to further investigate the receptor properties (Fig. 3B). The effective concentration, 50% [EC₅₀] of L-glutamate-activated currents was 0.4 mM (negative molar logarithm of molar EC₅₀ [pEC₅₀] = 3.4 ± 0.2). The Hill coefficient (n_H) for the L-glutamate response was 0.8 ± 0.3, revealing lack of positive cooperativity. L-glutamate-mediated responses were fully reversible and desensitized rapidly. The desensitization time course was dependent on the concentration of L-glutamate (SI Appendix, Fig. S4A). In the presence of 3 μM

L-glutamate, the time constant of desensitization (τ) was 1.3 ± 0.3 s. With 30 mM L-glutamate, the rate of desensitization was faster, with the time constant decreased to 0.6 ± 0.1 s. The I-V relationships for the glutamate-gated currents of *B. malayi* AVR-14B produced a reversal potential (E_{rev}) of -28.9 ± 2.9 mV, close to the Nernst potential of -24 mV for chloride ions in *Xenopus* oocytes (49) (SI Appendix, Fig. S4B).

Actions of PTX and fipronil (FIP). PTX is a naturally occurring poisonous crystalline phytochemical isolated from the fruit of *Anamirta cocculus* and related plants of the moonseed family. It is an equimolar mixture of picrotoxinin and picrotin, the latter being less active (50, 51). PTX is a prototypic antagonist of GABA receptors and inhibits anion flux in all other members of the ligand-gated chloride channel family (3, 52–59). FIP, a phenylpyrazole insecticide, is a potent GABA blocker and an inhibitor of GluCl (25, 60–64). We tested PTX and FIP (0.3 to 100 μM) as an agonist as well as an antagonist on the expressed *Bma*-AVR-14B channel. Both compounds failed to produce direct activation; however, when coapplied with 30 mM L-glutamate, concentration-dependent inhibition of the L-glutamate-gated currents was observed (Fig. 3C and D). At the highest concentration of 100 μM, PTX failed to completely block the glutamate-mediated currents while FIP produced ~95% inhibition of the glutamate response. Interestingly, we observed slight but nonsignificant potentiation of the glutamate currents in the presence of 0.3, 1, and 3 μM PTX. The IC₅₀ and n_H values for the coapplication of PTX and 30 mM L-glutamate were 33.1 μM (pIC₅₀ = 4.5 ± 0.2) and -1.2 ± 0.6, respectively (Fig. 3C). We observed that the inhibition produced by PTX was dose dependent and reversible. The IC₅₀ and n_H values for the coapplication of FIP and 30 mM L-glutamate were 1.8 μM (pIC₅₀ = 5.7 ± 0.1) and -1.3 ± 0.4, respectively (Fig. 3D). The inhibition of L-glutamate-induced currents by FIP was not completely reversible and was more potent in comparison to PTX.

Action of IVM. IVM activates native GluCl receptors of nematodes and stabilizes an open-channel conformation, generating inhibitory transmembrane currents in pharyngeal muscle cells and motor neurons (10, 21, 24, 26, 27, 34, 37, 65). In addition to gating the GluCl channels directly, IVM acts synergistically

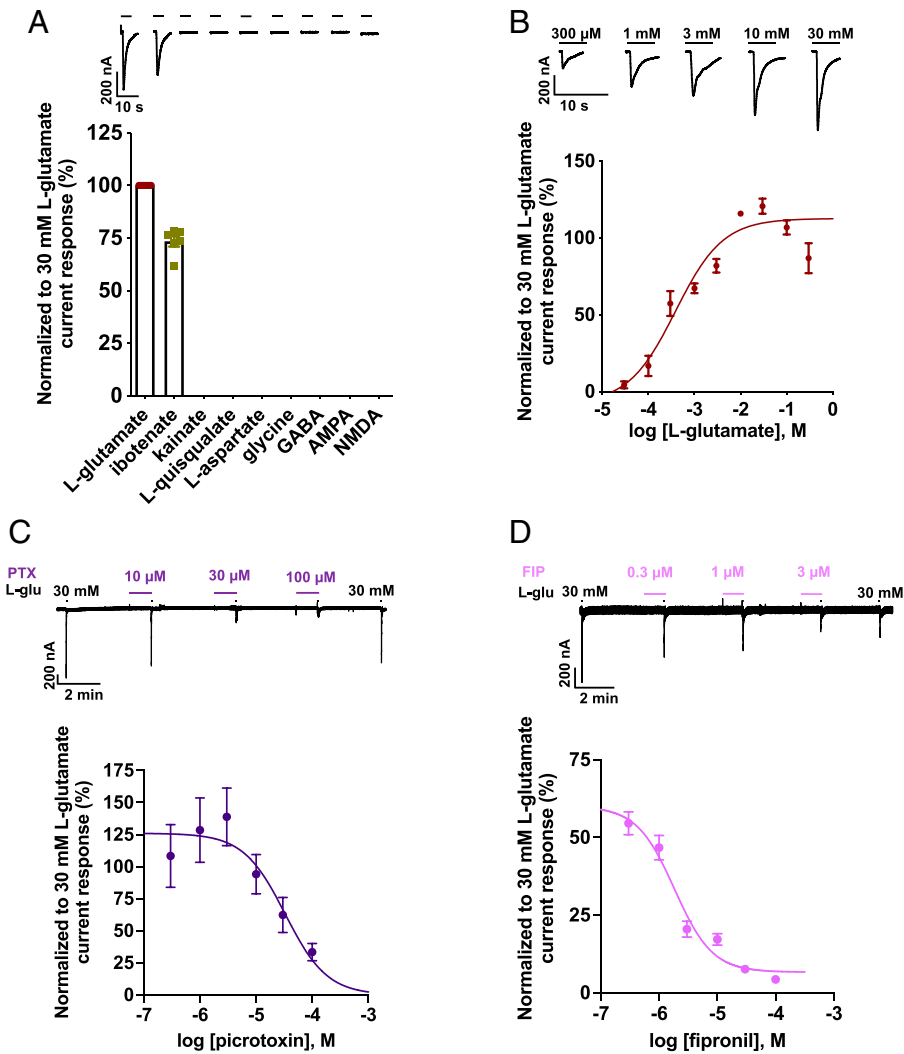


Fig. 3. Pharmacology of *B. malayi* AVR-14B. (A) Representative traces (Top) for agonist responses and bar chart (Bottom) showing mean \pm SEM, %, for normalized current responses to the different agonists tested at 1 mM. Rank order series: L-glutamate (100 ± 0.0 , $n = 13$) > ibotenate (73.4 ± 2.5 , $n = 6$) \gg kainate ($n = 6$) = L-quisqualate ($n = 6$) = L-aspartate ($n = 7$) = glycine ($n = 7$) = GABA ($n = 7$) = AMPA ($n = 7$) = NMDA ($n = 7$). (B) Representative inward current traces and concentration-response plot for L-glutamate ($n \geq 5$). L-glutamate produced an $EC_{50} = 0.4$ mM (pEC_{50} of 3.4 ± 0.2) and $n_H = 0.8 \pm 0.3$. (C) Representative trace (Top) and concentration-inhibition curve (Bottom) for L-glutamate (L-glu)-mediated response in the presence of PTX ($n = 5$). The IC_{50} and n_H values were $33.1 \mu\text{M}$ ($pIC_{50} = 4.5 \pm 0.2$) and -1.2 ± 0.6 . (D) Representative trace (Top) and concentration-inhibition curve (Bottom) for L-glutamate-mediated response in the presence of FIP ($n = 5$). The IC_{50} and n_H values were $1.8 \mu\text{M}$ ($pIC_{50} = 5.7 \pm 0.1$) and -1.3 ± 0.4 . L-glu, L-glutamate. Error bars in A–D represent SEM.

with glutamate, rendering the receptor susceptible to further activation by the natural ligand (7, 21, 58, 66). We examined the effects of IVM on oocytes expressing *Bma*-AVR-14B receptor. Fig. 4 A and B shows representative currents and cumulative concentration-response plot for IVM (10 pM to 1 μM) normalized to 30 mM glutamate-activated currents. IVM-sensitive inward currents were slowly activating, nondesensitizing, irreversible, and dose dependent. The analysis of the IVM concentration-response plot generated an EC_{50} of 1.9 nM ($pEC_{50} = 8.7 \pm 1.2$), with corresponding n_H values of 0.3 ± 0.1 . We also tested the effects of IVM (0.01 nM and 0.1 nM) on 100 μM , 1 mM, and 10 mM L-glutamate-gated currents to further characterize the pharmacology (Fig. 4 C–F). IVM failed to produce the characteristic potentiation of L-glutamate responses. In the presence of 0.1-nM concentration IVM, the current responses of all the concentrations of L-glutamate were significantly inhibited while 0.01 nM produced significant inhibition of 1-mM and 10-mM L-glutamate-mediated currents. This demonstrated that *Bma*-AVR-14B exhibits differences in IVM sensitivity in comparison to other nematode GluCl.

Action of NA. NA, a potent insecticidal fungal product, targets insect GluCl by a mechanism comparable to IVM. It is not a structural analog of IVM and directly activates chloride conductance of insect GluCl as well as potentiates channel opening by glutamate (21, 43–46, 67, 68). Its mechanism of action on nematode GluCl has not been elucidated yet. In Worminator motility experiments, NA produced inhibition of adult worm motility. We were also interested in determining the pharmacological effects of NA on the *Bma*-AVR-14B GluCl channels (Fig. 5). When examined as an agonist, NA-sensitive currents displayed slower activation kinetics than glutamate, similar to IVM, with an EC_{50} of 2.7 μM ($pEC_{50} = 5.6 \pm 0.2$) and n_H of 1.6 ± 0.8 (Fig. 5 A and D). To test the positive allosteric modulation (PAM) effects of NA, we examined the effect of different concentrations, 0.03 to 3 μM , of NA on 30- μM L-glutamate responses, since higher concentrations of NA produced significant agonist effects (Fig. 5 B and D). NA potentiated the L-glutamate-mediated currents, causing a left shift of the concentration-response curve and generating an estimated minimum EC_{50} of 0.4 μM ($pEC_{50} = 6.4 \pm 0.4$) and n_H of 0.8 ± 0.4 (Fig. 5D and *SI Appendix*,

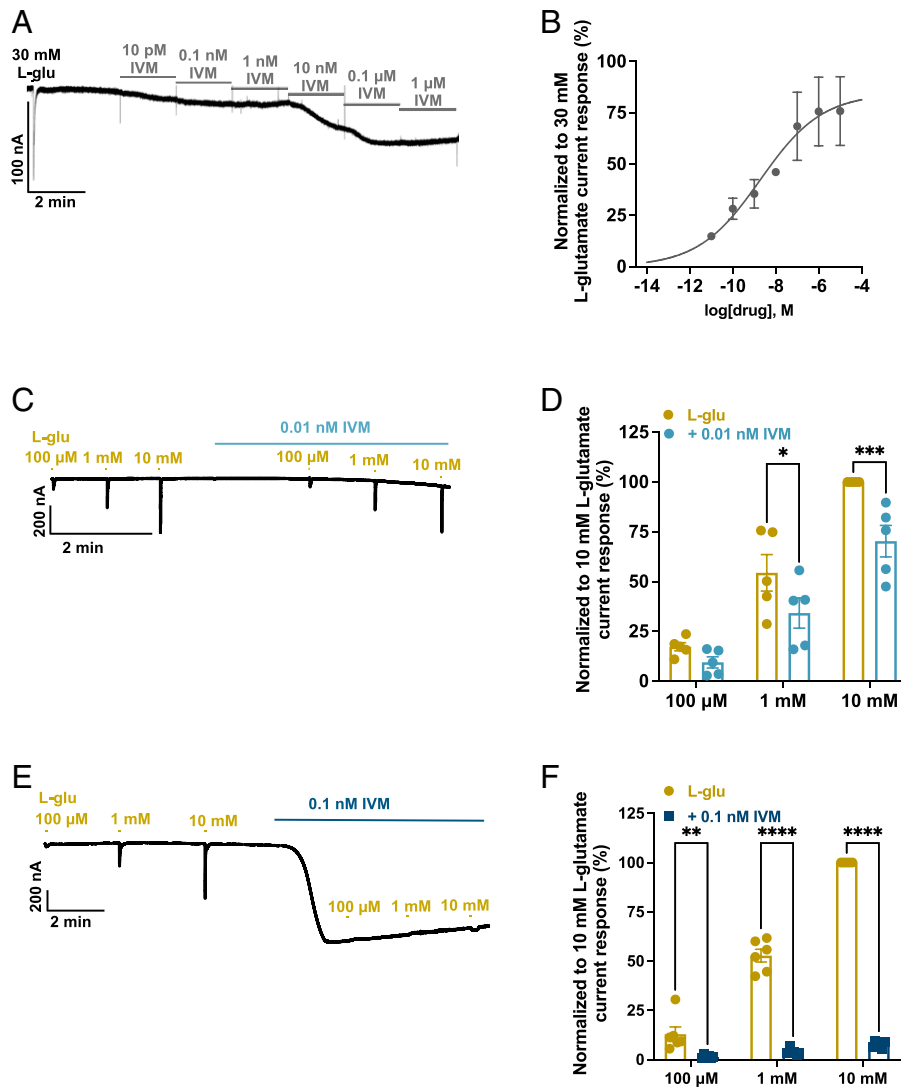


Fig. 4. Activation of *B. malayi* AVR-14B by IVM. (A) Representative trace showing the cumulative concentration-response relationship for IVM. (B) Cumulative concentration-response relationship curve for IVM. The EC_{50} and n_H values for IVM were 1.9 nM ($pEC_{50} = 8.7 \pm 1.2$) and 0.3 ± 0.2 . (C and D) Representative trace (C) and scatter plot (D) with bar showing the effect of 0.01 nM IVM ($n = 6$) on $100\text{-}\mu\text{M}$, 1-mM , and 10-mM L-glutamate-mediated current responses (expressed as mean \pm SEM, %; normalized to 10 mM L-glutamate response); 0.01 nM IVM produced significant inhibition of 1-mM (54.3 ± 9.2 alone; 34.2 ± 7.5 in the presence of IVM) and 10-mM (100.0 ± 0.0 alone; 70.3 ± 7.9) L-glutamate-mediated current responses. (E and F) Representative trace (E) and scatter plot (F) with bar showing the effect of 0.1 nM IVM ($n = 6$) on $100\text{-}\mu\text{M}$, 1-mM , and 10-mM L-glutamate-mediated current responses (mean \pm SEM %; normalized to 10-mM L-glutamate response); 0.1 nM IVM produced significant inhibition of $100\text{-}\mu\text{M}$ (12.9 ± 3.7 alone; 1.3 ± 0.3 in the presence of IVM), 1-mM (52.8 ± 3.3 alone; 4.0 ± 0.6 in the presence of IVM), and 10-mM (100.0 ± 0.0 alone; 7.7 ± 0.7 in the presence of IVM) L-glutamate-mediated current responses. Two-way ANOVA; $*P \leq 0.05$, $**P \leq 0.01$, $***P \leq 0.001$, $****P \leq 0.0001$; significantly different as indicated; Bonferroni's multiple comparisons tests. L-glu, L-glutamate. Error bars in B, D, and F represent SEM.

Fig. S5). NA not only increased the responses to L-glutamate but also decreased desensitization, which is characteristic of a type II PAM (69). To quantify this effect, we measured the area under the curve (AUC) for each of the experiments and plotted the concentration-response curves (Fig. 5E). In the presence of NA, an approximately sevenfold increase in the mean AUC response of L-glutamate was observed. Therefore, NA produces direct activation at higher concentrations (>3 μM) and acts as a potentiator of L-glutamate-gated responses at lower concentrations (<3 μM).

IVM acts as an inhibitor of NA-mediated potentiation of L-glutamate-gated currents. Our previous experiments had shown that IVM gated the *Bma*-AVR-14B chloride channel as a direct activator alone. Besides failing to exhibit the characteristic positive potentiation of the glutamate effects, IVM inhibited the chloride currents of the natural ligand in oocytes. In contrast, NA displayed both direct activation and positive potentiation of the glutamate effects on *Bma*-AVR-14B channels. To get a better mechanistic

understanding of *Bma*-AVR-14B channel properties, we next analyzed the effects of IVM on NA-mediated potentiation of L-glutamate responses. When tested at a moderately high concentration (0.1 nM), IVM activated the receptor and eliminated the agonist as well as PAM effects of NA (Fig. 6A and B). At a lower concentration (1 pM), IVM did not activate the *Bma*-AVR-14B receptor directly. As shown in Fig. 6C and D and *SI Appendix*, Fig. S6, 1 pM IVM produced a significant reduction of NA-mediated positive potentiation of L-glutamate AUC response with no significant shift in normalized current plot. This suggests that IVM acts as an inhibitor of NA-mediated pharmacological effects of *Bma*-AVR-14B GluCl receptors.

Discussion

GluCl α 3/AVR-14 subunit orthologs are conserved in all nematode genomes studied so far (2, 21, 28, 29, 32, 34, 65, 70, 71). *Avr-14* exhibits polymorphism and undergoes alternate splicing to yield

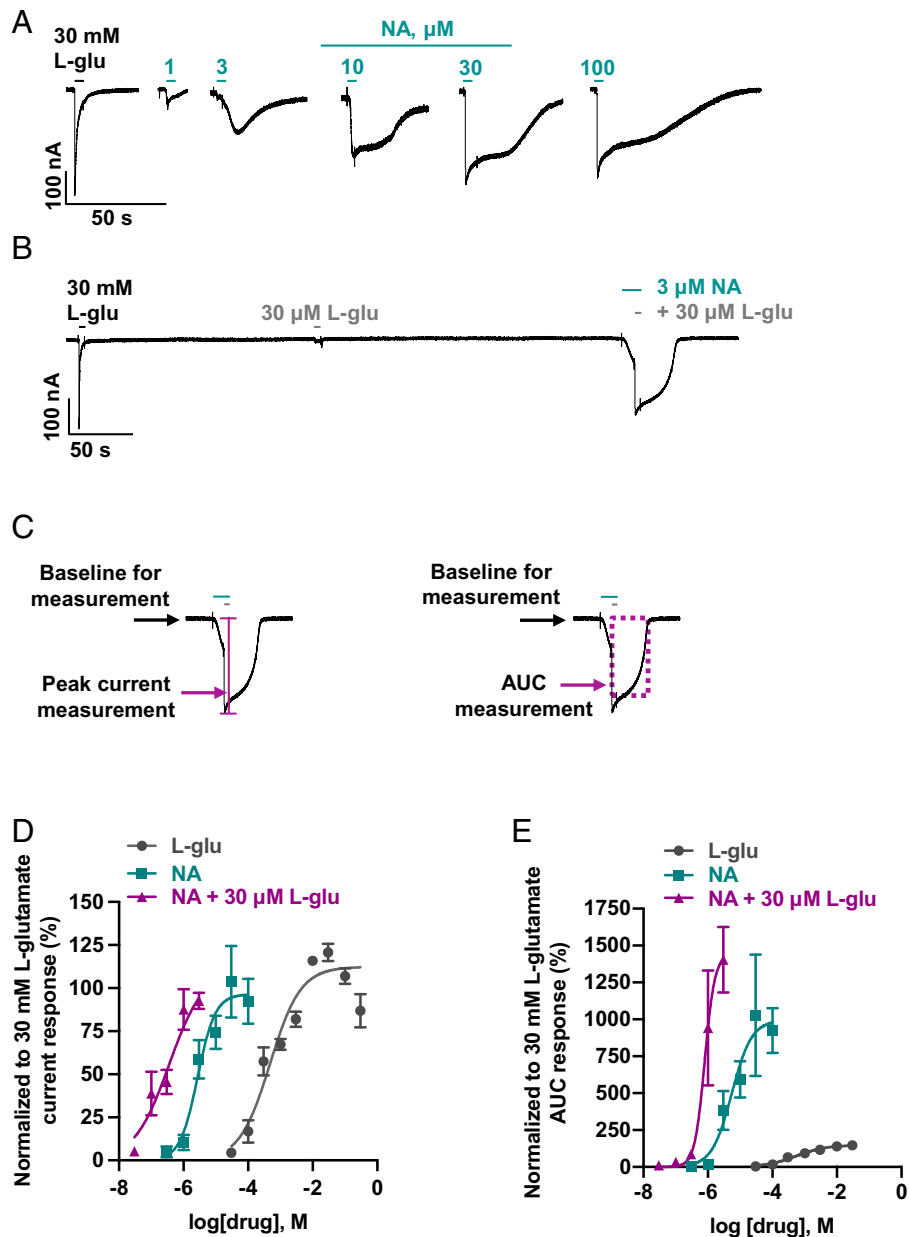


Fig. 5. Effect of NA on the *Xenopus* oocytes expressing *B. malayi* AVR-14B. (A) Representative inward current responses from oocyte challenged with increasing concentrations of NA ($n \geq 5$). (B) Representative inward current response from oocyte used for studying the positive modulatory effect of NA on L-glutamate (30 μ M) gated current response ($n \geq 5$). (C) Example of peak current and AUC measurements of the traces to quantify the PAM effect of NA on L-glutamate gated current response. (D) Concentration-response relationship curves for L-glutamate, NA, and NA in the presence of 30 μ M L-glutamate when normalized to 30-mM L-glutamate current response. EC_{50} and n_H were 0.4 mM ($pEC_{50} = 3.4 \pm 0.2$) and 0.8 ± 0.3 for L-glu, respectively; 2.7 μ M ($pEC_{50} 5.6 \pm 0.2$) and 1.6 ± 0.8 for NA, respectively. The estimated minimum EC_{50} and n_H for NA in the presence of 30 μ M L-glu was 0.4 μ M ($pEC_{50} = 6.4 \pm 0.4$) and 0.8 ± 0.4 , respectively. Bottom was constrained to zero. (E) Concentration-response relationship curves for L-glutamate, NA, and NA in the presence of 30 μ M L-glutamate when normalized to 30-mM L-glutamate AUC response. AUC (max) \pm SEM, %, was 154.7 ± 10.4 for L-glutamate; 999.4 ± 227.1 for NA; 1430.0 ± 168.3 for NA in the presence of 30 μ M L-glutamate. L-glu, L-glutamate. Error bars in D and E represent SEM.

two subunits in most nematode species, GluCl α 3A/AVR-14A and GluCl α 3B/AVR-14B, which differ in their C-terminal channel-forming domain (23, 33, 36, 40, 65, 72) (SI Appendix, Table S1). Mutations in the *avr-14* subunit have been associated with avermectin resistance in *C. elegans*, *Ostertagia ostertagi*, and *C. onchophora* and locomotory defects in *C. elegans*, which makes this subunit an important in vivo target for IVM in nematodes (32, 36, 65, 73). The expression pattern of *avr-14* varies with nematode species. In free-living nematode *C. elegans* and gastrointestinal nematodes, *avr-14* expression correlates well with the observed effects of IVM on pharyngeal pumping, motility, and fecundity (36, 41, 71, 74–76). In *C. elegans*, the gene is expressed in extrapharyngeal neurons in the head, ventral cord motor

neurons, hook neurons, and mechanosensory neurons, while in *H. contortus* expression has been reported in pharyngeal neurons, amphidial neurons, motor neuron commissures, lateral and ventral nerve cords, and nerve ring (36, 41, 71, 74, 75). In filarial nematodes, IVM produces microfilaricidal effects resulting in fast clearance of mf and prolonged suppression of mf production from adult females; however, it has limited macrofilaricidal activity (9). Several studies have shown reduced motility, impaired embryogenesis, and reduced mf output in filarial nematodes after exposure to IVM (77–81). In adult *B. malayi* worms, *avr-14* is highly expressed in reproductive tissues and embryos, which may account for the inhibitory effects of IVM on embryogenesis, suppression of mf production, and sterilizing effects in adult worms

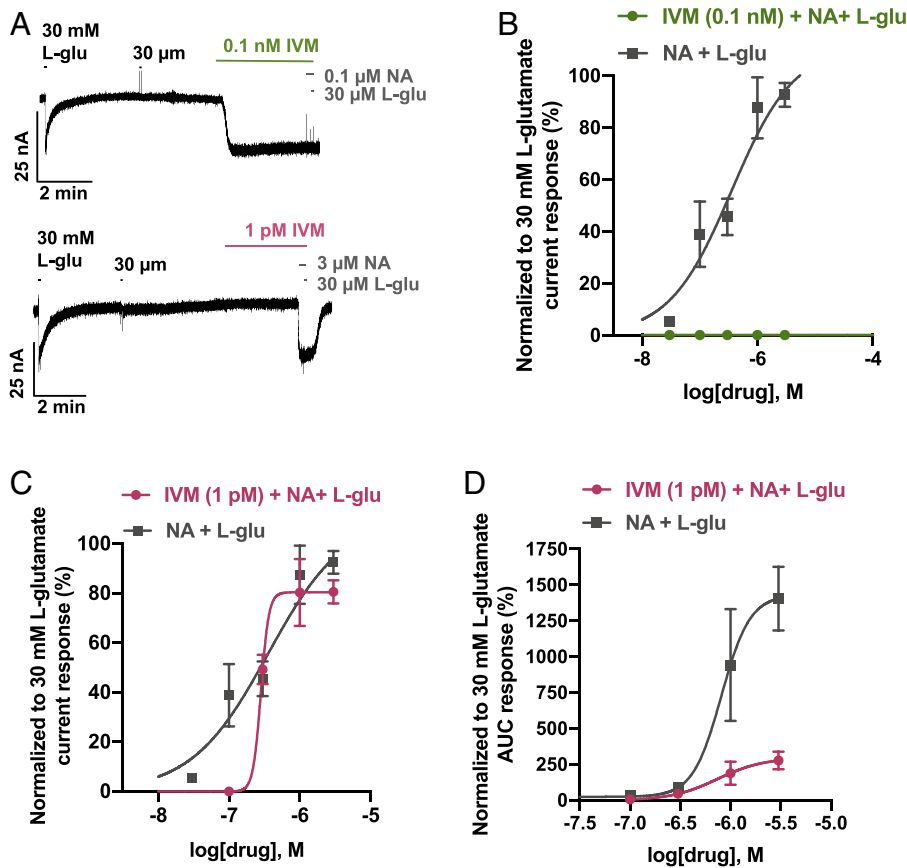


Fig. 6. IVM acts as an inhibitor of NA-mediated potentiation of L-glutamate-gated currents in the *Xenopus* oocytes expressing *B. malayi* AVR-14B. (A) Representative inward current responses showing the effect of IVM (0.1 nM IVM in top trace, $n = 6$; 1 pM in bottom trace; $n = 6$) on combination of NA with L-glutamate (L-glu; 30 μ M). (B) Concentration-response curves showing the potent inhibitory effect of 0.1 nM IVM on combination of NA (0.1 to 0.3 μ M) with L-glutamate (30 μ M) when normalized to 30-mM L-glutamate current response. (C) Concentration-response curves showing effect of 1 pM IVM on combination of NA (0.1 to 3 μ M) with L-glutamate (30 μ M) when normalized to 30-mM L-glutamate current response. EC_{50} values were 0.4 μ M ($pEC_{50} = 6.4 \pm 0.4$) for NA and L-glutamate combination in the absence of IVM; 0.3 μ M ($pEC_{50} = 6.5 \pm 1.0$) NA and L-glutamate combination in the presence of IVM. There was no significant difference between the Hill slopes. (D) Concentration-response curves showing effect of 1 pM IVM on combination of NA (0.1 to 3 μ M) with L-glutamate (30 μ M) when normalized to 30-mM L-glutamate AUC response. AUC (max) \pm SEM, %, was 1,430.0 \pm 168.3 for NA and L-glutamate combination in the absence of IVM; 295.5 \pm 101.0 for NA and L-glutamate combination in the presence of IVM. L-glu, L-glutamate. Error bars in B and C represent SEM.

(82). Moreno et al. (83) reported expression of *avr-14* in tissues surrounding the excretory–secretory (ES) pore of mf, which suggests that the GluCl expressed by this subunit regulates protein secretion from the ES pore. IVM exposure significantly reduced ES pore protein secretion that enables evasion of host’s immune response by targeting AVR-14 GluCl. The basis of lack of macrofilaricidal activity of IVM is not yet understood. It could be due to physiological differences, differential expression of GluCl in filarial nematodes in comparison to nonfilarial nematodes, diversity of GluCl channels, or variation in IVM sensitivity or pharmacology. We were interested in understanding the effects of IVM exposure on adult worm motility and the role of *avr-14* in regulating locomotory behavior. We performed Worminator motility assays and report sex-, concentration-, and time-dependent effects of IVM and NA on the motility of the *B. malayi* adult. Both compounds produced reduction in the motility of adult worms, with females being more sensitive to the effects. Anthelmintics, including emodepside, diethylcarbamazine (DEC), and levamisole, also exhibit inhibitory effects on *B. malayi* motility, but the effects are observed in minute time-scale (84–86). Levamisole and emodepside are significantly more potent than NA and IVM, with an IC_{50} in the nanomolar range ($IC_{50(female)} = 10$ nM for levamisole; $IC_{50(female)} = 801$ nM and $IC_{50(male)} = 176$ nM for emodepside), while DEC had a comparable IC_{50} of 4.4 μ M. However, both levamisole- and DEC-treated worms have a short-lasting sensitivity to these anthelmintics and show a gradual recovery from the paralytic effects within 3 to 4 h. In comparison, IVM- and NA-treated worms do not show any sign of recovery from the motility paralysis. RNA interference (RNAi) knockdown of *avr-14* in adult *B. malayi* produced a modest reduction in motility, demonstrating the physiological relevance of the subunit to worm fitness. However, the individual contribution of different AVR-14 isoforms to locomotory behavior in vivo

has yet to be fully resolved. The timescale for producing motility deficits was longer in comparison to drugs such as levamisole and emodepside (which act directly on the muscle or nerve of the parasite). While levamisole acts almost instantaneously by direct action on nematode muscle acetylcholine receptors (AChRs), GluCl activation in many nematodes causes pharyngeal paralysis, which leads to starvation and lack of energy sources, gradually reducing muscle contraction and movement over time. This is one possibility, but for microfilaria and other filarial worms, it is possible that motor neurons are involved. Furthermore, Li et al. (82) reported moderate levels of expression of *avr-14* in the lateral chord and somatic muscles of adult *B. malayi* worms. Taken together, we believe AVR-14 is physiologically and therapeutically relevant in *B. malayi*. However, AVR-14 may assemble with other GluCl subunits to form a heterooligomer to regulate locomotor behavior.

The molecular basis of the anthelmintic effect of IVM in filarial nematodes is not yet fully understood. In this study, we successfully expressed the AVR-14B GluCl from the filarial nematode *B. malayi*. Sequence analysis shows that *B. malayi* AVR-14B is a homolog of *C. elegans* AVR-14B/GluCl α 3B, *H. contortus* gbr-2B/GluCl α 3B, *D. immitis* AVR-14B/GluCl α 3B, and *C. oncophora* GluCl α 3 subunit (26, 32, 34, 36, 71) and shares high (>71%) amino acid identity. The *Bma*-AVR-14B subunit is assembled as a functional homomeric channel with pharmacological characteristics comparable to those previously characterized in nematode GluCl. The expressed GluCl channel produced rapidly desensitizing inward currents in the presence of L-glutamate and its conformationally constrained analog, ibotenate. L-glutamate produced dose-dependent and fully reversible responses and was more sensitive on *B. malayi* AVR-14B (EC_{50} of 0.4 mM) in comparison to *C. elegans* ($EC_{50} = 2.2$ mM) and *D. immitis* ($EC_{50} \sim 1$ mM). In contrast, *C. oncophora* ($EC_{50} = 29.7$ μ M in IVM-sensitive strain and $EC_{50} = 96.1$ μ M in IVM-resistant

strain) and *H. contortus* ($EC_{50} = 27.6 \mu\text{M}$) AVR-14B GluCl were activated by much lower concentrations of the natural ligand. Amino acid residues in the extracellular pretransmembrane 1 (TM1) region have been implicated in affecting the efficacy of glutamate (26, 28, 33). Both *H. contortus* and *C. oncophora* have a lysine (charged side chain) residue at position 254 and leucine (hydrophobic side chain) at position 256. These residues are replaced by valine (hydrophobic side chain at position 246) and arginine (charged side chain at position 248) in *C. elegans*, while *B. malayi* and *D. immitis* have methionine (hydrophobic side chain at position 242) and leucine (hydrophobic side chain at position 244) instead. It is possible that the lower sensitivity of L-glutamate seen in *B. malayi* is contributed by this part of the subunit. The biological significance of this decreased sensitivity of *Bma*-AVR-14B for L-glutamate is not yet known. One explanation is that the lower sensitivity of AVR-14B for L-glutamate helps in modulating the activity required for a particular physiological response. Another possibility is that AVR-14B assembles with other GluCl subunits as a heteromeric GluCl complex. Other agonists of vertebrate glutamate receptors and candidate amino acid neurotransmitters did not activate *Bma*-AVR-14B GluCl. The expressed AVR-14B chloride-selective channels were inhibited by FIP and PTX in a concentration-dependent manner, as observed in some of the corresponding orthologs from other nematodes.

IVM directly activated *B. malayi* AVR-14B channel conductance with a slow and irreversible channel opening, as it does for other nematode orthologs characterized so far. The EC_{50} for IVM was 1.8 nM, which is similar to *H. contortus* (estimated $EC_{50} = \sim 0.1 \pm 1.0$ nM) but more sensitive than *C. oncophora* AVR-14 (IVM sensitive strain $EC_{50} = 0.5 \mu\text{M}$; IVM-resistant strain $EC_{50} = 1.3 \mu\text{M}$). Based on the potent IVM effect in *B. malayi*, the AVR-14B receptor has a relatively high affinity for IVM. L-glutamate and IVM have different binding sites on the GluCl receptor. The IVM-binding site is located in the transmembrane domain, between TM3 and TM1 of two adjacent subunits, while glutamate occupies the classical agonist site at subunit interfaces (29, 87). IVM at low concentrations has been shown to potentiate the electrophysiological response to glutamate (6, 7, 21, 58, 66). These data suggest that glutamate and IVM interaction is complementary and possibly additive. In our experiments, the inward currents produced by L-glutamate in the presence of 0.1 nM IVM were not allosterically potentiated but were inhibited. This suggests that the *Brugia* AVR-14B receptor has novel properties and may contribute to the observed disparity in therapeutic effects of IVM in filarial nematodes compared with other parasitic nematode species. NA is an indole diterpene insecticidal agent derived from the endophytic fungus *Nodulisporium* sp. (43, 44, 67). In insects, the mode of action of NA and IVM involves direct activation and potentiation of GluCl opening by glutamate (21, 45, 46). In this study, NA also produced both direct activation and PAM effects on the nematode GluCl *Bma*-AVR-14B. Specifically, NA behaved as a type II PAM by altering the kinetics as well as potentiating the amplitude of glutamate-mediated currents. The PAM effects of NA were seen to be more potent (estimated minimum EC_{50} 0.4 μM) than its direct activation effects (EC_{50} 2.7 μM). These results demonstrate that low concentrations of NA reduce glutamate-induced receptor desensitization. In summation, the effect of NA on *Bma*-AVR-14B is comparable to that of IVM on nonfilarial nematode receptors; contrastingly, the effect of IVM on *Bma*-AVR-14B is different from the effect of IVM on nonfilarial nematode receptors.

Our results confirmed that both NA and IVM directly activate *B. malayi* AVR-14B GluCl, but the mechanisms of allosteric modulation are different. In contrast to glutamate, activation by

IVM or NA did not produce receptor desensitization. NA produced PAM when combined with glutamate. On the other hand, IVM inhibited glutamate-induced currents. We explored the effects of IVM on NA-mediated potentiation of glutamate-gated currents and found that IVM is an inhibitor of the PAM effects of NA. Smith et al. (45) reported similar inhibitory effects of IVM on binding of NA to insect GluCl and proposed the existence of multiple populations of receptors with different NA- and IVM-binding affinities; this was unlikely in our experiments, as we investigated a single population of homomeric receptors. Interestingly, when used at lower concentration (1 pM), IVM inhibited NA-mediated potentiation of the L-glutamate AUC response without any significant effect on the peak current response. These results suggest a complex interaction between IVM and NA. Atif et al. (66) reported that the *H. contortus* AVR-14B receptor oscillates between multiple functional states during activation by glutamate and IVM. Our proposed model states that binding of glutamate or NA shifts the receptor to the open state, while binding of IVM changes the GluCl receptor from the resting state to a lower conductance state (Fig. 7 A and B). In our model, there was no direct route to the open state from the lower conductance state once the receptor was bound by IVM. Also in our model, binding of NA and glutamate together produced type II PAM. This explains the inhibitory effects of IVM on the pharmacological effects of glutamate and NA on *B. malayi* AVR-14B GluCl.

In conclusion, we have shown that *Bma*-AVR-14B functionally expresses a homomeric GluCl in *Xenopus* oocytes and that these channels are gated by L-glutamate and ibotenate. The actions of L-glutamate on the filarial GluCl were concentration dependent and inhibited by PTX and FIP, with the latter being more potent. IVM acted as a direct activator of the AVR-14B receptor and also as a negative allosteric modulator (NAM) of glutamate-mediated currents. This contrasts with previously reported PAM effects of IVM on other nematode GluCl receptors. Our results show that NA has a complex mode of action on *Bma*-AVR-14B. At low concentrations (<10 μM), NA acts as a positive allosteric modulator of *Bma*-AVR-14B, and at high concentrations ($\geq 10 \mu\text{M}$), the drug acts as a direct activator of this receptor. Because the PAM effects of NA described in this study are characteristic of type II PAMs (potentiation of agonist effects and decrease in desensitization), it may constitute a suitable backbone for structure-activity relationship studies to facilitate the development of GluCl PAMs as potential filaricidal drugs that are effective on adult parasites. It is worth noting that the effects of IVM on our expressed receptor occurred at much lower concentrations than the effects observed on motility in our studies. In contrast, effects on the expressed receptor and adult motility observed using NA all fell within a similar (low μM) concentration range. It is tempting to argue that the effects on motility by NA are aligned with the PAM effects of the drug (missing in IVM treatments). Our study shows that *Bma*-AVR-14 has unusual pharmacological properties, with IVM behaving as a NAM while NA exhibits PAM effects similar to those reported for IVM on GluCl from other nematodes. These results suggest that GluCl remain valid targets for new anthelmintics effective against adult filarial parasites.

Materials and Methods

Parasite Maintenance. Adult *B. malayi* worms were obtained from the NIH/National Institute of Allergy and Infectious Diseases (NIAID) Filariasis Research Reagent Resource Center (College of Veterinary Medicine, University of Georgia, Athens, GA) and were maintained in L-glutamine containing nonphenol red Roswell Park Memorial Institute (RPMI) 1640 media (Life Technologies)

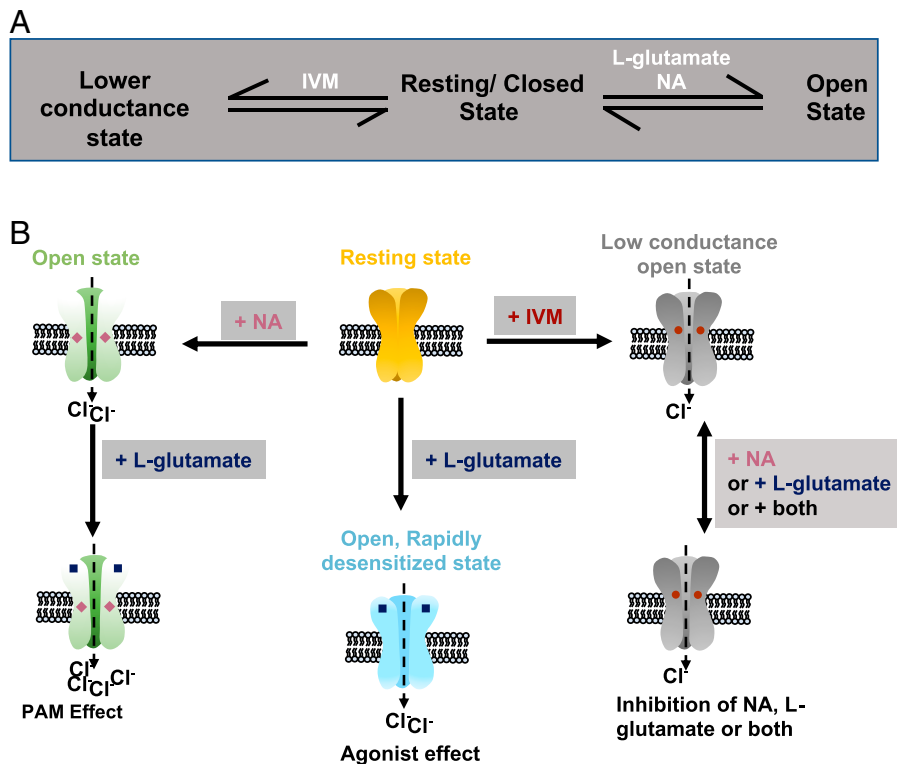


Fig. 7. (A) Schematic showing the multiple states of *Bma-AVR-14B* receptor after ligand binding. (B) Diagrammatic representation of the ligand-binding model for *Bma-AVR-14B* receptor.

supplemented with 10% heat-inactivated fetal bovine serum (Thermo Fisher Scientific) and 1% penicillin-streptomycin (Life Technologies). The worms were placed in an incubator at 37 °C supplemented with 5% CO₂.

B. malayi Motility Analysis. The worms were separated in 24-well plates with 1 mL RPMI media, and motility analysis was done using the Worminator system as described in ref. 88. The drugs, NA and IVM, were dissolved in dimethyl sulfoxide (DMSO; (final concentration 0.1% [vol/vol])). For concentration-response analysis, drugs were added to the well, and motility was recorded at different time points after treatment with WormAssay v1.4. Control worms were treated with 0.1% DMSO. RNAi experiments were performed using *Bma-avr-14* target dsRNA. LacZ dsRNA served as off target control and deoxyribonuclease/riboNuclease-free water was used as negative control. dsRNA was synthesized as explained in Kashyap et al. (84) and McCoy et al. (89). Target PCR products were amplified using the primers shown in *SI Appendix, Table S2*. T7-labeled PCR products were generated using the overhang T7 promoter sequence 5'-TAA TACGACTCACTATAG-3'. RiboMAX Express RNAi kit (Promega) was used to synthesize dsRNA. Adult *B. malayi* were soaked in RPMI media containing 30 to 60 μg/mL of target and control dsRNA. Worms not used in the motility assay were snap frozen in liquid nitrogen and stored at -80 °C for transcript analysis by qPCR. WormAssay v1.4 was used to record the movement of worms at different time points after dsRNA treatment. The % Motility was calculated as a percentage ratio of motility of worms after treatment at each time point over motility of naive worms.

Cloning of *B. malayi* AVR-14B. Three adult female worms were used for total RNA extraction using TRIzol Reagent (Invitrogen). RT-PCR was used to synthesize *B. malayi* complementary DNA (cDNA) using both oligo(dT)₁₂₋₁₈ Primer and SuperScript IV VIL0 Master Mix (Invitrogen). The cDNA served as template for PCR amplification of full-length coding sequence of the putative *B. malayi* *avr-14B* (GenBank: HQ123447.1, without the 5' untranslated region atgaatggtgt) using Phusion High Fidelity DNA Polymerase (Thermo Fisher Scientific). Specific primers containing *KpnI* (*gggtacc*; 5' end of the forward primer) and *Apal* (*gggccc*; 3' end of the reverse primer) restriction enzyme sites were designed for PCR amplification of *Bma-avr-14b* (forward primer: 5'-AAAggtaccACCACC ATGATTTGTTGATTTTAC-3'; reverse primer: 5'-AAAgggcccTCAATTCACATAATTCACA TAG-3'). Kozac motif (CCACC) was added to the forward primer for optimal translation of *Bma-avr-14B*. PCR products were digested with *KpnI* and *Apal* restriction

enzymes, followed by gel-purification using the NucleoSpin Gel and PCR Cleanup kit (Macherey-Nagel Inc.) and were then cloned into pTB207 expression vector. The cloned constructs were sequenced with pTB207 vector primers (forward, T7) and (reverse, SP6) for confirmation of positive clones, which were used for capped RNA (cRNA) synthesis using the T7 mMessage mMachine in vitro transcription kit (Invitrogen). Agarose gel (1%) was used to check the quality of cRNA, and quantification was done by absorption microscopy. Subsequently, cRNA was aliquoted and stored at -80 °C.

***X. laevis* Oocyte Microinjection and Two-Electrode Voltage-Clamp Electrophysiology (TEVC).** De-folliculated oocytes obtained from Ecoocyte Bioscience were used for heterologous expression of *Bma-AVR-14B* as previously described (90, 91). Briefly, the oocytes were injected with 15 to 55 ng of *Bma-AVR-14B* cRNA in 41 to 50 nL nuclease-free water. cRNA was injected in the animal pole of the oocytes using a nanoject II microinjector (Drummond Scientific). The injected oocytes were incubated at 19 °C for 5 to 7 d in 96-well plates containing 300 μL incubation solution/well (88 mM NaCl, 1 mM KCl, 0.4 mM CaCl₂·2H₂O, 0.33 mM Ca(NO₃)₂, 0.8 mM MgSO₄, 5 mM Tris-HCl, 2.4 mM NaHCO₃, 2.5 mM Na pyruvate, 100 U/mL penicillin, and 100 μg/mL streptomycin, pH 7.4), one oocyte/well of 96-well culture plates. The solution was changed daily to keep the oocytes healthy. We performed TEVC recordings from oocytes expressing *Bma-AVR-14B* as described (90, 92). Noninjected oocytes served as the negative control. We used an $n \geq 4$ for each set of experiments. An Axoclamp 2B amplifier (Warner Instruments) was used to clamp the oocytes at -80 mV unless otherwise stated. Data were acquired on a desktop computer with Clampex 10.2 (Molecular Devices). Oocytes were impaled with microelectrodes that were pulled using a Flaming/Brown horizontal electrode puller (Model P-97; Sutter Instruments). The microelectrodes were filled with 3 M KCl, and their tips were carefully broken with tissue paper to attain a low resistance of 2 to 5 MΩ in recording solution [100 mM NaCl, 2.5 mM KCl, 1 mM CaCl₂·2H₂O, and 5 mM 4-(2-hydroxyethyl)-1-piperazineethanesulphonic acid, pH 7.3].

Chemicals. We purchased L-glutamate, L-aspartate, glycine, GABA, AMPA, NMDA, IVM, PTX, and FIP from Sigma-Aldrich. Ibotenate, kainate, and quisqualate were purchased from Tocris Bioscience (Bio-Techne Corp.). NA was a kind gift from Bayer Animal Health (Leverkusen, Germany). All chemicals except

IVM, PTX, and FIP (DMSO; final concentration $\leq 0.1\%$) were dissolved in recording solution.

Drug Applications. For agonist experiments, L-glutamate, L-aspartate, glycine, GABA, AMPA, NMDA, ibotenate, kainate, and quisqualate were tested at an initial concentration of 1 mM. Each chemical was applied for 5 s, followed by a wash-off period of 3 min with recording solution between applications to minimize the effects of desensitization. The concentration-response relationship for L-glutamate was generated by applying a control 5-s application of 30 mM L-glutamate, followed by increasing concentrations of L-glutamate (30 μ M to 30 mM) for 5 s with a wash-off interval of 3 min between each application. Since desensitization was observed as a feature of the AVR-14B receptor, we limited the L-glutamate concentrations applied to each oocyte to four; that is, for one set of oocytes, we applied 0.03, 0.3, 3, and 30 mM L-glutamate after the control 30-mM L-glutamate application. For the second set of oocytes, we applied 0.1, 1, 10, and 30 mM L-glutamate following the control 30-mM L-glutamate application. For the third set of oocytes, we applied 30, 100, and 300 mM L-glutamate following the control 30-mM L-glutamate application. The I-V relationship of responses to L-glutamate was determined by challenging each oocyte with repeated applications of 1 mM L-glutamate over a voltage range of -80 to $+20$ mV; 1 mM glutamate was first applied for 5 s with the membrane of the oocyte clamped -80 mV and followed by a 3-min wash with recording solution. A 1-mM glutamate application was then repeated at -60 , -40 , -20 , 0 , and $+20$ mV, and a 3-min wash-off was allowed between drug applications. Concentration-response relationships for ibotenate were generated by a 5-s application of increasing concentrations of ibotenate from 30 μ M to 30 mM. The oocytes were first challenged with a control 30 mM L-glutamate application for 5 s, followed by 5-s application of increasing concentrations of ibotenate. A 3-min wash-off interval was allowed between L-glutamate and ibotenate applications. The IVM cumulative concentration-response relationship study was performed by first applying a control 30 mM L-glutamate for 5 s, followed by a 3-min wash-off with recording solution and then 2-min cumulative applications of increasing concentrations of IVM from 10 pM to 1 μ M. For the allosteric modulation experiment with IVM, oocytes were first challenged with three different L-glutamate concentrations (100 μ M, 1 mM, and 10 mM) for 5 s each. A 3-min wash-off interval with recording solution was allowed after each L-glutamate application. This was followed by a test concentration of IVM (0.1 nM and 0.01 nM) for >3 min, immediately followed by a 5-s coapplication of 100 μ M, 1 mM, and 10 mM L-glutamate and IVM. A 3-min wash with recording solution was allowed after each coapplication of L-glutamate and IVM. For both agonist and PAM experiments with NA, one oocyte was tested per NA concentration because NA was shown to cause a rapid desensitization of the AVR-14B receptor in preliminary studies. For the concentration-response relationship experiment, a control 30 mM L-glutamate was first applied for 5 s, followed by perfusion with recording solution for 3 min and then a 10-s application of a single concentration of NA/oocyte. This procedure was repeated for all NA concentrations (0.3 to 30 μ M). For PAM experiments with NA, oocytes were first challenged with a control 30 mM L-glutamate application for 5 s, followed by 3-min

recording solution perfusion, after which 30 μ M L-glutamate was applied for 5 s. This was followed by a 3-min wash with recording solution and a 10-s application of a single NA concentration prior to a 5-s coapplication of 30 μ M L-glutamate and NA. We tested five different concentrations of NA (0.03, 0.1, 0.3, 1, and 3 μ M) for these electrophysiology recordings. For antagonist experiments with PTX and FIP, oocytes were first challenged with a control 30 mM L-glutamate application for 5 s, after which recording solution was perfused for 3 min, followed by a 1-min application of antagonist prior to a 5-s coapplication of 30 mM L-glutamate and antagonist. This procedure was repeated with increasing concentrations (0.3 to 100 μ M) of the test antagonist, and a 3-min wash with recording solution was allowed between all applications. Only three concentrations of PTX or FIP were tested per oocyte to minimize the effects of desensitization. We applied 0.3, 1, and 3 μ M PTX or FIP following the control 30-mM L-glutamate application for one set of oocytes, and for another set of oocytes, we applied 10, 30, and 100 μ M PTX or FIP following the control 30-mM L-glutamate application.

Data Analysis. Data were analyzed using Clampfit 10.2 (Molecular Devices) and GraphPad Prism 9.3.1 (Graphpad Software Inc.). The data for sigmoid concentration-response curves was fitted to the Hill equation. We used one-way ANOVA, two-way ANOVA, and two-tailed *t* test to test statistical differences (statistically different if $P < 0.05$). Bonferroni's multiple comparisons test was used as post hoc test. For agonist rank order series experiments, peak current responses to agonist application were normalized to the 1-mM L-glutamate response. For L-glutamate, ibotenate, NA, and IVM concentration-response experiments, peak currents evoked following drug applications were normalized to the initial 30-mM L-glutamate application. For antagonist experiments, peak current responses to coapplication of antagonist and 30 mM L-glutamate were normalized to the control 30-mM L-glutamate response at the start of each experiment.

The authors acknowledge that subsections of *Materials and Methods* were modified from the creative component "Functional expression of a glutamate-gated chloride channel (GLC-3) from adult *Brugia malayi*" (93) previously produced by our lab.

Data, Materials, and Software Availability. All study data are included in the article and/or *SI Appendix*.

ACKNOWLEDGMENTS. This project was supported by a grant from Bayer Animal Health GmbH, Monheim, Germany, and by Grants R21 AI092185/AI/NIAID, R21 AI125899/AI/NIAID, and R01 AI047194/AI/NIAID from the NIH to R.J.M. and A.P.R.

1. T. Lynagh *et al.*, Molecular basis for convergent evolution of glutamate recognition by pentameric ligand-gated ion channels. *Sci. Rep.* **5**, 8558 (2015).
2. D. F. Cully, H. Wilkinson, D. K. Vassiliatis, A. Etter, J. P. Arena, Molecular biology and electrophysiology of glutamate-gated chloride channels of invertebrates. *Parasitology* **113** (suppl.), S191-S200 (1996).
3. T. A. Cleland, Inhibitory glutamate receptor channels. *Mol. Neurobiol.* **13**, 97-136 (1996).
4. D. K. Vassiliatis *et al.*, Evolutionary relationship of the ligand-gated ion channels and the avermectin-sensitive, glutamate-gated chloride channels. *J. Mol. Evol.* **44**, 501-508 (1997).
5. A. K. Jones, D. B. Sattelle, The cys-loop ligand-gated ion channel gene superfamily of the nematode, *Caenorhabditis elegans*. *Invert. Neurosci.* **8**, 41-47 (2008).
6. R. J. Martin, An electrophysiological preparation of *Ascaris suum* pharyngeal muscle reveals a glutamate-gated chloride channel sensitive to the avermectin analogue, milbemycin D. *Parasitology* **112**, 247-252 (1996).
7. D. J. Brownlee, L. Holden-Dye, R. J. Walker, Actions of the anthelmintic ivermectin on the pharyngeal muscle of the parasitic nematode, *Ascaris suum*. *Parasitology* **115**, 553-561 (1997).
8. A. Cook *et al.*, *Caenorhabditis elegans* ivermectin receptors regulate locomotor behaviour and are functional orthologues of *Haemonchus contortus* receptors. *Mol. Biochem. Parasitol.* **147**, 118-125 (2006).
9. T. G. Geary, Y. Moreno, Macrocyclic lactone anthelmintics: Spectrum of activity and mechanism of action. *Curr. Pharm. Biotechnol.* **13**, 866-872 (2012).
10. R. J. Martin, A. P. Robertson, S. Choudhary, Ivermectin: An anthelmintic, an insecticide, and much more. *Trends Parasitol.* **37**, 48-64 (2021).
11. V. Raymond, D. B. Sattelle, Novel animal-health drug targets from ligand-gated chloride channels. *Nat. Rev. Drug Discov.* **1**, 427-436 (2002).
12. R. J. Martin, Modes of action of anthelmintic drugs. *Vet. J.* **154**, 11-34 (1997).
13. M. Abongwa, R. J. Martin, A. P. Robertson, A brief review on the mode of action of antinematodal drugs. *Acta Vet. (Beogr.)* **67**, 137-152 (2017).
14. J. P. Arena *et al.*, The mechanism of action of avermectins in *Caenorhabditis elegans*: Correlation between activation of glutamate-sensitive chloride current, membrane binding, and biological activity. *J. Parasitol.* **81**, 286-294 (1995).
15. J. C. Chabala *et al.*, Ivermectin, a new broad-spectrum antiparasitic agent. *J. Med. Chem.* **23**, 1134-1136 (1980).
16. B. M. Greene, K. R. Brown, H. R. Taylor, "Use of ivermectin in humans" in *Ivermectin and Abamectin*, W. C. Campbell, Ed. (Springer, New York, NY, 1989), pp. 311-323.
17. C. L. Haber *et al.*, Development of a mechanism of action-based screen for anthelmintic microbial metabolites with avermectinlike activity and isolation of milbemycin-producing *Streptomyces* strains. *Antimicrob. Agents Chemother.* **35**, 1811-1817 (1991).
18. A. Crump, S. Omura, Ivermectin, 'wonder drug' from Japan: The human use perspective. *Proc. Jpn. Acad. Ser. B Phys. Biol. Sci.* **87**, 13-28 (2011).
19. B. Colatrella, The Mectizan Donation Program: 20 Years of successful collaboration - A retrospective. *Ann. Trop. Med. Parasitol.* **102** (suppl. 1), 7-11 (2008).
20. R. W. Burg *et al.*, Avermectins, new family of potent anthelmintic agents: Producing organism and fermentation. *Antimicrob. Agents Chemother.* **15**, 361-367 (1979).
21. D. F. Cully *et al.*, Cloning of an avermectin-sensitive glutamate-gated chloride channel from *Caenorhabditis elegans*. *Nature* **371**, 707-711 (1994).
22. A. Etter, D. F. Cully, J. M. Schaeffer, K. K. Liu, J. P. Arena, An amino acid substitution in the pore region of a glutamate-gated chloride channel enables the coupling of ligand binding to channel gating. *J. Biol. Chem.* **271**, 16035-16039 (1996).

23. J. A. Dent, M. W. Davis, L. Avery, *avr-15* encodes a chloride channel subunit that mediates inhibitory glutamatergic neurotransmission and ivermectin sensitivity in *Caenorhabditis elegans*. *EMBO J.* **16**, 5867–5879 (1997).
24. D. K. Vassiliatis *et al.*, Genetic and biochemical evidence for a novel avermectin-sensitive chloride channel in *Caenorhabditis elegans*. Isolation and characterization. *J. Biol. Chem.* **272**, 33167–33174 (1997).
25. L. Horoszok, V. Raymond, D. B. Sattelle, A. J. Wolstenholme, GLC-3: A novel fipronil and BIDN-sensitive, but picrotoxinin-insensitive, L-glutamate-gated chloride channel subunit from *Caenorhabditis elegans*. *Br. J. Pharmacol.* **132**, 1247–1254 (2001).
26. S. McCavera, A. T. Rogers, D. M. Yates, D. J. Woods, A. J. Wolstenholme, An ivermectin-sensitive glutamate-gated chloride channel from the parasitic nematode *Haemonchus contortus*. *Mol. Pharmacol.* **75**, 1347–1355 (2009).
27. C. L. Cheeseman, N. S. Delany, D. J. Woods, A. J. Wolstenholme, High-affinity ivermectin binding to recombinant subunits of the *Haemonchus contortus* glutamate-gated chloride channel. *Mol. Biochem. Parasitol.* **114**, 161–168 (2001).
28. A. J. Wolstenholme, A. T. Rogers, Glutamate-gated chloride channels and the mode of action of the avermectin/milbemycin anthelmintics. *Parasitology* **131** (suppl.), S85–S95 (2005).
29. A. J. Wolstenholme, Glutamate-gated chloride channels. *J. Biol. Chem.* **287**, 40232–40238 (2012).
30. K. L. Mealey, Therapeutic implications of the MDR-1 gene. *J. Vet. Pharmacol. Ther.* **27**, 257–264 (2004).
31. A. H. Schinkel *et al.*, Disruption of the mouse *mdr1a* P-glycoprotein gene leads to a deficiency in the blood-brain barrier and to increased sensitivity to drugs. *Cell* **77**, 491–502 (1994).
32. A. I. Njue, J. Hayashi, L. Kinne, X. P. Feng, R. K. Prichard, Mutations in the extracellular domains of glutamate-gated chloride channel $\alpha 3$ and β subunits from ivermectin-resistant *Cooperia oncophora* affect agonist sensitivity. *J. Neurochem.* **89**, 1137–1147 (2004).
33. D. M. Yates, A. J. Wolstenholme, An ivermectin-sensitive glutamate-gated chloride channel subunit from *Dirioflaria immitis*. *Int. J. Parasitol.* **34**, 1075–1081 (2004).
34. D. F. Cully, P. S. Pares, K. K. Liu, J. M. Schaeffer, J. P. Arena, Identification of a *Drosophila melanogaster* glutamate-gated chloride channel sensitive to the antiparasitic agent ivermectin. *J. Biol. Chem.* **271**, 20187–20191 (1996).
35. S. G. Forrester, R. K. Prichard, R. N. Beech, A glutamate-gated chloride channel subunit from *Haemonchus contortus*: Expression in a mammalian cell line, ligand binding, and modulation of anthelmintic binding by glutamate. *Biochem. Pharmacol.* **63**, 1061–1068 (2002).
36. J. A. Dent, M. M. Smith, D. K. Vassiliatis, L. Avery, The genetics of ivermectin resistance in *Caenorhabditis elegans*. *Proc. Natl. Acad. Sci. U.S.A.* **97**, 2674–2679 (2000).
37. M. Pellegrino, "Association between GLC-4 and AVR-14: Role of GluCl subunit composition in *Caenorhabditis elegans* ivermectin sensitivity and behavior," PhD thesis, McGill University, Montreal, Canada (2003).
38. S. G. Forrester, R. K. Prichard, J. A. Dent, R. N. Beech, *Haemonchus contortus*: HcGluCl α expressed in *Xenopus* oocytes forms a glutamate-gated ion channel that is activated by isbotenate and the antiparasitic drug ivermectin. *Mol. Biochem. Parasitol.* **129**, 115–121 (2003).
39. S. G. Forrester, F. F. Hamdan, R. K. Prichard, R. N. Beech, Cloning, sequencing, and developmental expression levels of a novel glutamate-gated chloride channel homologue in the parasitic nematode *Haemonchus contortus*. *Biochem. Biophys. Res. Commun.* **254**, 529–534 (1999).
40. S. M. Williamson, T. K. Walsh, A. J. Wolstenholme, The cys-loop ligand-gated ion channel gene family of *Brugia malayi* and *Trichinella spiralis*: A comparison with *Caenorhabditis elegans*. *Invert. Neurosci.* **7**, 219–226 (2007).
41. V. Portillo, S. Jagannathan, A. J. Wolstenholme, Distribution of glutamate-gated chloride channel subunits in the parasitic nematode *Haemonchus contortus*. *J. Comp. Neurol.* **462**, 213–222 (2003).
42. R. N. Beech, A. J. Wolstenholme, C. Neveu, J. A. Dent, Nematode parasite genes: What's in a name? *Trends Parasitol.* **26**, 334–340 (2010).
43. D. A. Ostlind *et al.*, Discovery of a novel indole diterpene insecticide using first instars of *Lucilia sericata*. *Med. Vet. Entomol.* **11**, 407–408 (1997).
44. P. T. Meinke, M. M. Smith, W. L. Shoop, Nodulisporic acid: Its chemistry and biology. *Curr. Top. Med. Chem.* **2**, 655–674 (2002).
45. M. M. Smith *et al.*, Nodulisporic acid opens insect glutamate-gated chloride channels: Identification of a new high affinity modulator. *Biochemistry* **39**, 5543–5554 (2000).
46. S. W. Ludmerer *et al.*, Ivermectin and nodulisporic acid receptors in *Drosophila melanogaster* contain both γ -aminobutyric acid-gated Rdl and glutamate-gated GluCl α chloride channel subunits. *Biochemistry* **41**, 6548–6560 (2002).
47. W. N. Green, C. P. Wanamaker, The role of the cysteine loop in acetylcholine receptor assembly. *J. Biol. Chem.* **272**, 20945–20953 (1997).
48. T. Grutter *et al.*, Molecular tuning of fast gating in pentameric ligand-gated ion channels. *Proc. Natl. Acad. Sci. U.S.A.* **102**, 18207–18212 (2005).
49. N. Dascal, The use of *Xenopus* oocytes for the study of ion channels. *CRC Crit. Rev. Biochem.* **22**, 317–387 (1987).
50. G. A. R. Johnston *et al.*, "Herbal products and GABA receptors" in *Encyclopedia of Neuroscience*, L. R. Squire, Ed. (Academic Press, Oxford, 2009), pp. 1095–1101.
51. E. Hodgson, "Toxins and venoms" in *Progress in Molecular Biology and Translational Science*, E. Hodgson, Ed. (Academic Press, 2012), vol. **112**, chap. 14.
52. R. W. Olsen, Picrotoxin-like channel blockers of GABA_A receptors. *Proc. Natl. Acad. Sci. U.S.A.* **103**, 6081–6082 (2006).
53. A. Etter *et al.*, Picrotoxin blockade of invertebrate glutamate-gated chloride channels: Subunit dependence and evidence for binding within the pore. *J. Neurochem.* **72**, 318–326 (1999).
54. C. F. Newland, S. G. Cull-Candy, On the mechanism of action of picrotoxin on GABA receptor channels in dissociated sympathetic neurons of the rat. *J. Physiol.* **447**, 191–213 (1992).
55. K. W. Yoon, D. F. Covey, S. M. Rothman, Multiple mechanisms of picrotoxin block of GABA-induced currents in rat hippocampal neurons. *J. Physiol.* **464**, 423–439 (1993).
56. H. Qian, Y. Pan, Y. Zhu, P. Khalili, Picrotoxin accelerates relaxation of GABA_A receptors. *Mol. Pharmacol.* **67**, 470–479 (2005).
57. J. D. Goutman, D. J. Calvo, Studies on the mechanisms of action of picrotoxin, quercetin and pregnanolone at the GABA_A1 receptor. *Br. J. Pharmacol.* **141**, 717–727 (2004).
58. J. P. Arena, K. K. Liu, P. S. Pares, J. M. Schaeffer, D. F. Cully, Expression of a glutamate-activated chloride current in *Xenopus* oocytes injected with *Caenorhabditis elegans* RNA: Evidence for modulation by avermectin. *Brain Res. Mol. Brain Res.* **15**, 339–348 (1992).
59. I. Pribilla, T. Takagi, D. Langosch, J. Bormann, H. Betz, The atypical M2 segment of the beta subunit confers picrotoxinin resistance to inhibitory glycine receptor channels. *EMBO J.* **11**, 4305–4311 (1992).
60. T. Narahashi, X. Zhao, T. Ikeda, V. L. Salgado, J. Z. Yeh, Glutamate-activated chloride channels: Unique fipronil targets present in insects but not in mammals. *Pestic. Biochem. Physiol.* **97**, 149–152 (2010).
61. X. Zhao, J. Z. Yeh, V. L. Salgado, T. Narahashi, Fipronil is a potent open channel blocker of glutamate-activated chloride channels in cockroach neurons. *J. Pharmacol. Exp. Ther.* **310**, 192–201 (2004).
62. M. E. Scharf, B. D. Siegfried, Toxicity and neurophysiological effects of fipronil and fipronil sulfone on the western corn rootworm (Coleoptera: Chrysomelidae). *Arch. Insect Biochem. Physiol.* **40**, 150–156 (1999).
63. T. Narahashi, Nerve membrane ion channels as the target site of insecticides. *Mini Rev. Med. Chem.* **2**, 419–432 (2002).
64. T. Ikeda, X. Zhao, Y. Kono, J. Z. Yeh, T. Narahashi, Fipronil modulation of glutamate-induced chloride currents in cockroach thoracic ganglion neurons. *Neurotoxicology* **24**, 807–815 (2003).
65. A. I. Njue, R. K. Prichard, Genetic variability of glutamate-gated chloride channel genes in ivermectin-susceptible and -resistant strains of *Cooperia oncophora*. *Parasitology* **129**, 741–751 (2004).
66. M. Atif, A. Estrada-Mondragon, B. Nguyen, J. W. Lynch, A. Keramidis, Effects of glutamate and ivermectin on single glutamate-gated chloride channels of the parasitic nematode *H. contortus*. *PLoS Pathog.* **13**, e1006663 (2017).
67. N. S. Kane *et al.*, Drug-resistant *Drosophila* indicate glutamate-gated chloride channels are targets for the antiparasitics nodulisporic acid and ivermectin. *Proc. Natl. Acad. Sci. U.S.A.* **97**, 13949–13954 (2000).
68. J. G. Ondeyka *et al.*, Nodulisporic acid A, a novel and potent insecticide from a *Nodulisporium* Sp. isolation, structure determination, and chemical transformations. *J. Am. Chem. Soc.* **119**, 8809–8816 (1997).
69. M. S. Thomsen, J. D. Mikkelsen, Type I and II positive allosteric modulators differentially modulate agonist-induced up-regulation of $\alpha 7$ nicotinic acetylcholine receptors. *J. Neurochem.* **123**, 73–83 (2012).
70. T. H. M. Mes, Purifying selection and demographic expansion affect sequence diversity of the ligand-binding domain of a glutamate-gated chloride channel gene of *Haemonchus placei*. *J. Mol. Evol.* **58**, 466–478 (2004).
71. S. Jagannathan *et al.*, Ligand-gated chloride channel subunits encoded by the *Haemonchus contortus* and *Ascaris suum* orthologues of the *Caenorhabditis elegans* gbr-2 (avr-14) gene. *Mol. Biochem. Parasitol.* **103**, 129–140 (1999).
72. D. L. Laughton, G. G. Lunt, A. J. Wolstenholme, Alternative splicing of a *Caenorhabditis elegans* gene produces two novel inhibitory amino acid receptor subunits with identical ligand binding domains but different ion channels. *Gene* **201**, 119–125 (1997).
73. A. El-Abdellati *et al.*, Altered *avr-14B* gene transcription patterns in ivermectin-resistant isolates of the cattle parasites, *Cooperia oncophora* and *Ostertagia ostertagi*. *Int. J. Parasitol.* **41**, 951–957 (2011).
74. P. A. Correa, T. Gruninger, L. R. Garcia, DOP-2 D2-like receptor regulates UNC-7 innexins to attenuate recurrent sensory motor neurons during *C. elegans* copulation. *J. Neurosci.* **35**, 9990–10004 (2015).
75. S. K. Glendinning, S. D. Buckingham, D. B. Sattelle, S. Wonnacott, A. J. Wolstenholme, Glutamate-gated chloride channels of *Haemonchus contortus* restore drug sensitivity to ivermectin resistant *Caenorhabditis elegans*. *PLoS One* **6**, e22390 (2011).
76. T. G. Geary *et al.*, *Haemonchus contortus*: Ivermectin-induced paralysis of the pharynx. *Exp. Parasitol.* **77**, 88–96 (1993).
77. J. B. Tompkins, L. E. Stitt, B. F. Ardelli, *Brugia malayi*: In vitro effects of ivermectin and moxidectin on adults and microfilariae. *Exp. Parasitol.* **124**, 394–402 (2010).
78. S. K. Tagboto, S. Townson, *Onchocerca volvulus* and *O. lienalis*: The microfilaricidal activity of moxidectin compared with that of ivermectin in vitro and in vivo. *Ann. Trop. Med. Parasitol.* **90**, 497–505 (1996).
79. G. Strote, S. Wieland, K. Darge, J. C. W. Comley, In vitro assessment of the activity of anthelmintic compounds on adults of *Onchocerca volvulus*. *Acta Leiden.* **59**, 285–296 (1990).
80. W. A. Stolk *et al.*, Effects of ivermectin and diethylcarbamazine on microfilariae and overall microfilaria production in bancroftian filariasis. *Am. J. Trop. Med. Hyg.* **73**, 881–887 (2005).
81. P. Tippawangkosol *et al.*, Comparative assessment of the in vitro sensitivity of *Brugia malayi* infective larvae to albendazole, diethylcarbamazine and ivermectin alone and in combination. *Southeast Asian J. Trop. Med. Public Health* **35** (suppl. 2), 15–21 (2004).
82. B. W. Li, A. C. Rush, G. J. Weil, High level expression of a glutamate-gated chloride channel gene in reproductive tissues of *Brugia malayi* may explain the sterilizing effect of ivermectin on filarial worms. *Int. J. Parasitol. Drugs Drug Resist.* **4**, 71–76 (2014).
83. Y. Moreno, J. F. Nabhan, J. Solomon, C. D. Mackenzie, T. G. Geary, Ivermectin disrupts the function of the excretory-secretory apparatus in microfilariae of *Brugia malayi*. *Proc. Natl. Acad. Sci. U.S.A.* **107**, 20120–20125 (2010).
84. S. S. Kashyap *et al.*, Anthelmintic resistance and homeostatic plasticity (*Brugia malayi*). *Sci. Rep.* **11**, 14499 (2021).
85. S. S. Kashyap *et al.*, Emodepside has sex-dependent immobilizing effects on adult *Brugia malayi* due to a differentially spliced binding pocket in the RCK1 region of the SLO-1 K channel. *PLoS Pathog.* **15**, e1008041 (2019).
86. S. Verma, S. S. Kashyap, A. P. Robertson, R. J. Martin, Diethylcarbamazine activates TRP channels including TRP-2 in filaria, *Brugia malayi*. *Commun. Biol.* **3**, 398 (2020).
87. R. E. Hibbs, E. Gouaux, Principles of activation and permeation in an anion-selective Cys-loop receptor. *Nature* **474**, 54–60 (2011).
88. C. Marcellino *et al.*, WormAssay: A novel computer application for whole-plate motion-based screening of macroscopic parasites. *PLoS Negl. Trop. Dis.* **6**, e1494 (2012).
89. C. J. McCoy *et al.*, RNA interference in adult *Ascaris suum*—an opportunity for the development of a functional genomics platform that supports organism-, tissue- and cell-based biology in a nematode parasite. *Int. J. Parasitol.* **45**, 673–678 (2015).
90. M. Abongwa *et al.*, Pharmacological profile of *Ascaris suum* ACR-16, a new homomeric nicotinic acetylcholine receptor widely distributed in *Ascaris* tissues. *Br. J. Pharmacol.* **173**, 2463–2477 (2016).
91. S. Choudhary *et al.*, Menthol acts as a positive allosteric modulator on nematode levamisole sensitive nicotinic acetylcholine receptors. *Int. J. Parasitol. Drugs Drug Resist.* **9**, 44–53 (2019).
92. S. Choudhary *et al.*, Pharmacological characterization of a homomeric nicotinic acetylcholine receptor formed by *Ancylostoma caninum* ACR-16. *Invert. Neurosci.* **19**, 11 (2019).
93. B. Akanjii, M. Abongwa, R. Martin, A. Robertson, Functional expression of a glutamate-gated chloride channel (GLC-3) from adult *Brugia malayi*. <https://dr.lib.iastate.edu/entities/publication/09aca46-7cc0-4b6b-90e1-37891ea70f41>. Accessed 21 December 2021.